Mobility of Voltage-dependent Ion Channels and Lectin Receptors in the Sarcolemma of Frog Skeletal Muscle

RICHARD E. WEISS, WILLIAM M. ROBERTS,
WALTER STÜHMER, and WOLFHARD ALMERS

From the Department of Physiology and Biophysics, University of Washington, Seattle, Washington 98195

ABSTRACT The mobility of lectin receptors and of two types of ion channels was studied in skeletal muscles of the frog *Rana temporaria*. Lectin receptors were labeled with fluorescent derivatives of succinyl–concanavalin A (Con A) or wheat germ agglutinin (WGA), and their mobility was measured by fluorescence recovery after photobleaching. Of the receptors for WGA, ~53% were free to diffuse in the plane of the membrane, with an average diffusion coefficient as found in other preparations ($D = 6.4 \times 10^{-11}$ cm^2/s). Con A receptors were not measurably mobile. The mobility of voltage-dependent Na and K (delayed rectifier) channels was investigated with the loose-patch clamp method, coupled with through-the-pipette photodestruction of channels by ultraviolet (UV) light. Na channels were not measurably mobile ($D \leq 10^{-12}$ cm^2/s). With K channels, photodestruction was followed by a small but consistent recovery of K current, which suggested that some K channels diffused in the plane of the membrane. Our results with K currents are best fit if 25% of the K channels diffuse with $D = 5 \times 10^{-11}$ cm^2/s, with the remainder being immobile. For both Na and K channels, photodestruction by UV was most effective at a wavelength of ~289 nm. At this wavelength, the energy density required for an e-fold reduction in the number of functional channels was 0.40 J/cm^2 for Na channels and 0.94 J/cm^2 for K channels. Irradiation at this wavelength and dose did not measurably diminish the mobility of WGA receptors; hence, the immobility of Na and most K channels is not due to UV irradiation. It is concluded that mobile and immobile membrane proteins coexist in the sarcolemma of frog skeletal muscle, and that voltage-dependent Na and K channels are singled out for immobilization.

INTRODUCTION

In fully differentiated cells taken from adult animals, the mobility of integral membrane proteins in the plane of the cell membrane varies over a wide range. In most cases, the diffusion coefficient, D, is much lower than the value of 1–4 $\times 10^{-9}$ cm^2/s (Frye and Edidin, 1970; Poo and Cone, 1974; Liebman and Entine, 1974; Tank et al., 1982) expected if integral membrane proteins could diffuse freely in a fluid lipid bilayer (Saffman and Delbruck, 1975); this indicates that the mobility of most integral membrane proteins is restricted. An extreme example is the acetylcholine (ACh) receptor at the neuromuscular junction, whose mobility is so low ($<10^{-12}$ cm^2/s, Axelrod et al., 1976b; possibly $<10^{-14}$ cm^2/s, Almers and Stirling, 1984) that it cannot be detected with current methods. In an innervated adult muscle cell, ACh receptors are strictly confined to the small area directly beneath the innervating nerve terminal (Miledi, 1960; Fertuck and Salpeter, 1976), even though they survive there for weeks (Bevan and Steinbach, 1983). Immobility is clearly essential if ACh receptors are to remain concentrated at the endplate region throughout the life of the cell. ACh receptors are probably held in place by being anchored to components of the cytoskeleton (Tank et al., 1982), as is apparently the case with other integral membrane proteins in postsynaptic membranes (Gulley and Reese, 1981; Hirokawa and Heuser, 1982).

Voltage-dependent ion channels, such as Na and K channels of nerve and muscle, are also kept at discrete locations in the cell membrane of many cells (Almers and Stirling, 1984). In skeletal muscle, for instance, Na channels show a patchy distribution on the sarcolemma (Almers et al., 1983), are found at especially high concentration at the endplate region (Beam et al., 1985; Roberts and Almers, 1985), and are also prevented from entering the transverse tubular system at the same density as on the sarcolemma (Jaimovitch et al., 1976; Campbell and Hille, 1976; Almers et al., 1982). This uneven distribution suggests that Na channels are restricted in their mobility. To measure the mobility of voltage-dependent ion channels in cell membranes, a method was developed that combined local patch-clamp recording of membrane current with through-the-pipette photodestruction of ion channels by ultraviolet (UV) light. This method yielded the result that Na channels in the sarcolemma are essentially immobile, and hence must be anchored in the sarcolemma (Stühmer and Almers, 1982). An advantage of the technique is that it directly assays function. Furthermore, it does not rely on fluorescent labels that might themselves influence mobility and, in any case, may not be readily available for all ion channels.

In this paper, the mobility of voltage-dependent K channels is investigated. Most K channels were found to be immobile or severely restricted in their mobility, while there was a large population of relatively mobile lectin receptors. Tests of our method are reported, and comparison mobility measurements for membrane proteins other than ion channels are provided. We conclude that mobile and immobile membrane proteins coexist in the sarcolemma of skeletal muscle, and that Na and K channels are among the proteins that are singled out for immobilization. Our results help to explain how a muscle cell maintains the unequal distribution of these two channels over sarcolemma and the transverse

tubular system. Preliminary accounts of this work have been given (Weiss et al., 1984*a, b*, 1985).

METHODS

Fluorescence Recovery After Photobleaching (FRAP)

The method followed that of Peters et al. (1974), Edidin et al. (1976), Jacobsen et al. (1976), and Axelrod et al. (1976*b*).

Preparation. Small bundles of two to three fibers, or single fibers (70–100 µm diam) were dissected in Ringer fluid (composition: 115 mM NaCl, 2.5 mM KCl, 1.8 mM $CaCl_2$, 3 mM Na-phosphate buffer, pH 7.2) from semitendinosus muscles of *Rana temporaria*, mounted on plastic coverslips with fine silk threads tied to the tendon ends, and placed in 10-ml petri dishes for labeling with fluorescein-conjugated derivatives of wheat germ agglutinin (FITC-WGA) or succinyl–concanavalin A (FITC-sConA). Fluorescent lectins were obtained from US Biochemical Co., Cleveland, OH. The fibers were labeled during a 20–40-min incubation in a Ringer fluid (20°C) containing 25–60 µg/ml FITC-WGA or 1.7 µg/ml FITC-sConA, washed three times in lectin-free Ringer, taken off the plastic coverslips, and transferred to the experimental chamber (Fig. 1*B*). The fibers were mounted at 120% slack length and with the central 5 mm resting on a glass pedestal. On either side of the fibers lay glass microspheres (Duke Scientific, Palo Alto, CA), 62 µm ± 3.2% SD in diameter, which were held in place on the pedestal by vaseline. A glass or quartz coverslip was then placed on top of the fibers and fixed in place by two drops of dental wax (Dentsply Ltd., Weybridge, Surrey, England). This compressed the fibers slightly and resulted in an optically flat region of sarcolemma just beneath the coverslip. The microspheres acted as spacers and prevented the coverslip from compressing the fiber to a thickness of less than ~60 µm. The lectin-free experimental medium, usually a Ca-free, ATP-containing solution (relaxing solution, containing 96 mM K, 42 mM Na, 7.3 mM Mg, 112 mM morpholinopropanesulfonate, 15.8 mM propionate, 5.5 mM ATP, 15.6 mM creatine phosphate, 20 mM EGTA, pH 7.0) was then substituted for Ringer fluid; thereafter the fiber was ready for use.

Recording. Fluorescein was excited with 390–490-nm light and its fluorescence was observed at 510–600 nm with a Leitz Dialux microscope (E. Leitz, Inc., Rockleigh, NJ) fitted for epifluorescence. A schematic of the light path is shown in Fig. 1*A*. The excitation light was provided by a mercury arc (Osram HBO-100) in a lamp housing fitted with a quartz condenser (both from Oriel Co., Stamford, CT). The light passed through an electronic shutter (Uniblitz, Vincent Associates, Rochester, NY), a heat-absorbing filter, a neutral density filter, a 400-nm long-pass glass filter (Schott Optical Glass, Inc., Duryea, PA), and an interference filter into the epifluorescence port of the Leitz microscope. Except for the dichroic mirror, all lenses and filters were removed from the epifluorescence attachment. The filter cube directed the light through the microscope objective (Leitz 50× water immersion objective, 1.00 NA, a Nikon 100× glycerol immersion objective, 1.30 NA, or a 74× UV-transmitting reflecting objective, 0.65 NA, by R. & J. Beck, Watford, England) onto the preparation. In most experiments, the excitation beam also passed through a pinhole in the image plane of the objective (FS in Fig. 1*A*) to project a 3.6–7.2-µm-diam circular spot on the surface of the muscle fiber. The arrangement allowed us to excite and hence to sample fluorescence from a small, well-defined area of sarcolemma centered in the field of view. For local photobleaching of the fluorophore, the excitation beam could be temporarily intensified by removing the neutral density filter.

The fluorescence from the muscle fiber was measured by the photomultiplier tube in

a Nikon UFX camera unit (Nikon, Inc., Garden City, NY). The photomultiplier was sensitive only to light emitted from the central area covering 1% of the field of view. The camera unit was modified to provide electrical access to the output of the operational amplifier that measured the current from the photomultiplier anode. This output, which was a linear function of light intensity, was amplified, filtered (100 Hz four-pole Bessel), and passed to the A/D converter of a NOVA 3 computer (Data General Co., Westboro,
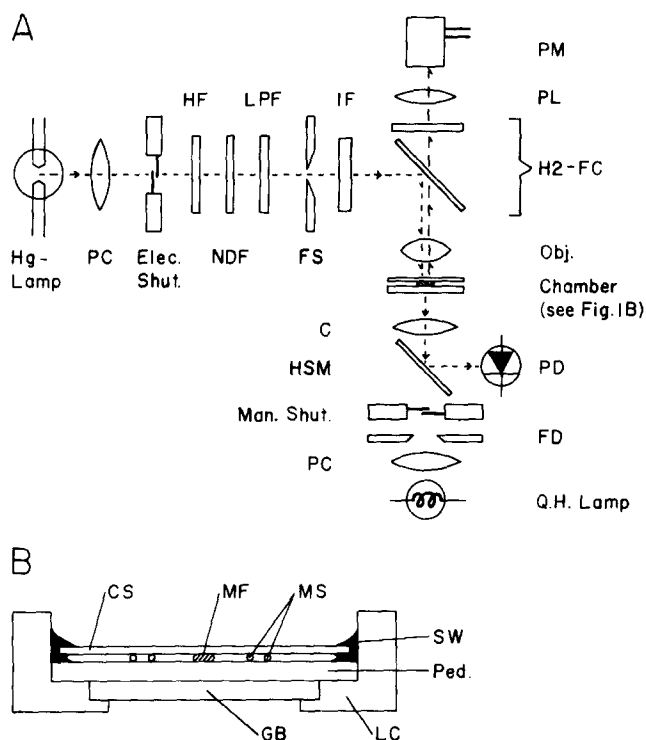

FIGURE 1.   (A) The light paths used in FRAP experiments. Abbreviations are: Hg lamp, mercury arc lamp; PC, primary condenser; elect. shut., electronic shutter; HF, heat filter; NDF, neutral density filter; LPF, long-pass (>400 nm) filter; FS, field stop; IF, interference filter; H2-FC, dichroic mirror with long-pass barrier filter; PL, projection lens; PM, photomultiplier; obj., microscope objective; C, condenser; HSM, half-silvered mirror; PD, photodiode; man. shut., manual shutter; FD, field diaphragm; Q.H. lamp, quartz halogen incandescent lamp. (B) The experimental chamber used in FRAP experiments. Abbreviations are: LC, Lucite chamber; GB, glass bottom; ped., glass pedestal; MS, microspheres (62 μm diam); CS, coverslip; SW, dental wax; MF, muscle fiber.

MA). The excitation light passing through the preparation and the microscope condenser was deflected by a half-silvered mirror onto an HUV 400B photodiode (EG&G, Salem, MA) so that intensity fluctuations of the excitation beam could be measured. The computer alternately sampled the outputs of the photomultiplier (fluorescent light) and the photodiode (excitation light), each at 5 kHz.

During a typical experiment, fluorescence measurements were made once every 30 s with a 10–100-fold-attenuated excitation beam. Immediately after photobleaching, the

frequency of measurement was temporarily increased to 10/min. The electronic shutter opened for 80 ms during each fluorescence measurement. 25 ms after the shutter had opened, the computer began to take samples, 250 each of excitation and fluorescent light. After the 50-ms sampling period was complete, the shutter closed. The computer calculated average values for the intensities of excitation and fluorescence emission during the 50-ms interval and calculated the fluorescence intensity (in arbitrary units) as the ratio of fluorescence emission and excitation intensity. Forming this ratio corrected for fluctuations in the excitation light intensity.

In some experiments, fibers were irradiated with UV light. The UV spectral lines from the mercury arc were selected with the appropriate bandpass interference filters and passed to the preparation through a reflecting objective. The interference filters had a 10-nm bandwidth at half-maximal intensity and were purchased from Ditric Optics Co., Marlboro, MA, or from Melles-Griot Co., Irvine, CA.
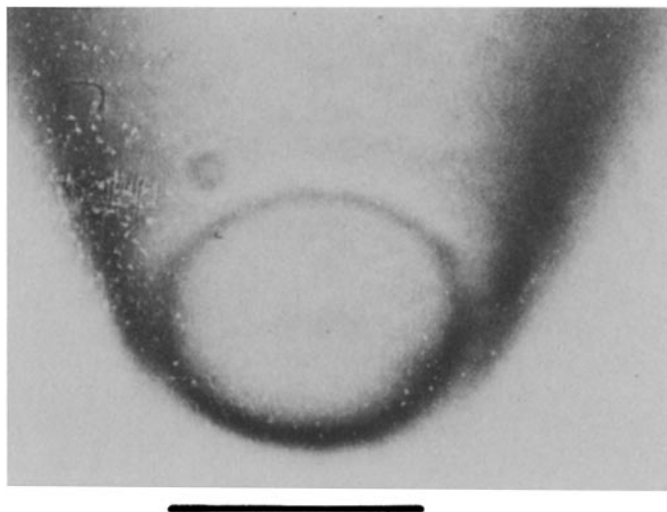

FIGURE 2.   The tip of the micropipette used in the experiment shown in Fig. 9, viewed at ~45° with respect to the shank axis. Calibration bar, 10 μm.

Electrical Recording

The muscle cell membrane was voltage-clamped with the loose-seal patch clamp (Almers et al., 1983) using circuitry described previously (Stühmer et al., 1984). Briefly, fire-polished glass pipettes of 11–30 μm tip diameter (Fig. 2) were pressed against sartorius muscle fibers of *R. temporaria* to electrically isolate a patch of sarcolemma. Suction was not applied to the pipette, and we avoided the region of the motor endplate. The resistance of the seal between pipette and membrane (R_s) was always greater than the pipette resistance (R_p, typically 0.15–0.3 MΩ), and was monitored throughout the experiment. Step depolarizations of 4.5 ms duration were applied to the pipette in order to elicit local currents I_{Na} and I_K through Na and K channels, respectively. Unless otherwise indicated, step amplitudes were 130 mV for measuring I_K and 90 mV for measuring peak I_{Na}. Na and K currents served as an assay for the number of functional Na and K channels in the patch. The holding potential was set to zero, i.e., equal to the resting potential of the fiber. Current recordings were corrected for capacitative and leakage currents by a

combination of digital and analog techniques, filtered (10 kHz low-pass, four-pole Bessel), and stored by the computer.

Unless the resting potential of the fiber is measured with a microelectrode, the absolute membrane potential is unknown in loose-patch experiments. However, the resting potential could be estimated from the voltage dependence of Na current activation. In order to exclude depolarized (and hence unhealthy) fibers, data were accepted only if the peak Na current during a 50-mV depolarizing step was <10% of that measured during a 90-mV step.

Local destruction of Na and K channels in the patch was achieved by directing UV light through the pipette and onto the patch of membrane beneath the pipette tip (Stühmer and Almers, 1982). The light from the mercury arc lamp, after passing through a UV bandpass interference filter, was focused onto one end of a 1-mm-diam quartz fiber (Math Associates, Port Washington, NY) by a 15× reflecting objective (R. & J. Beck); the other end of the quartz fiber was abutted against the back end of the pipette. Pipettes were coated to within 50 μm of the tip with an opaque epoxy paint to improve their electrical properties and also to minimize leakage of UV light through the glass wall. To measure the light emerging from the pipette, the tip was passed through a pinhole covering a photodiode (HUV 4000, EG&G). Experiments were rejected if, after UV irradiation, the inward current for a 130-mV step exceeded that for a 90-mV step; this was considered an indication of an unacceptably large rim current (Almers et al., 1983).

Unless indicated otherwise, all experiments were carried out at room temperature (22°C). Error bars represent 1 SEM.

RESULTS

Labeling of the Sarcolemma with FITC-WGA

WGA is a 35,000-mol-wt dimeric lectin that binds to N-acetyl-D-glucosamine and N-acetylneuraminic acid residues (Nagata and Burger, 1974). In a variety of cell culture lines, most WGA receptors have been shown to represent glycosylated integral membrane proteins (see Nicolson, 1974, for review). Fig. 3 shows photomicrographs of an isolated single fiber stained with FITC-WGA. The plane of focus led through the center of the fiber, and striations are clearly visible in transmitted light (Fig. 3A). When the fiber was viewed with fluorescence optics, it appeared that fluorescence was restricted to the edge of the fiber, which indicates that the lectin was bound to the fiber surface (Fig. 3B).

In Fig. 4, the microscope was focused onto the top surface of the fiber, providing a grazing view of the sarcolemma. Under bright-field illumination (Fig. 4A), faint striations from superficial sarcomeres are visible just below the cell membrane. Also visible is the nucleus of a small cell, probably a satellite cell, that was attached to the surface of this fiber. Fig. 4B was recorded with fluorescence optics. Although the fluorescence from the fiber surface appears granular or somewhat patchy, there were no completely dark areas. Evidently FITC-WGA was bound everywhere on the fiber surface. The outline of the small cell whose nucleus is visible in Fig. 4A appeared brightly. This cell was probably almost entirely within the microscope's plane of focus, since its membrane, labeled with fluorescent WGA, can be seen in edge view.

When the fluorescence of a small spot on the fiber surface was monitored using a photomultiplier and the protocol of repeated measurements described in

Methods, the fluorescence was found to remain undiminished for at least 3 h (not shown), even if the fiber was perfused with a bathing fluid that contained no FITC-WGA but had an excess (100 μg/ml) of unlabeled WGA. Evidently FITC-WGA remains stably associated with the sarcolemma for hours. The
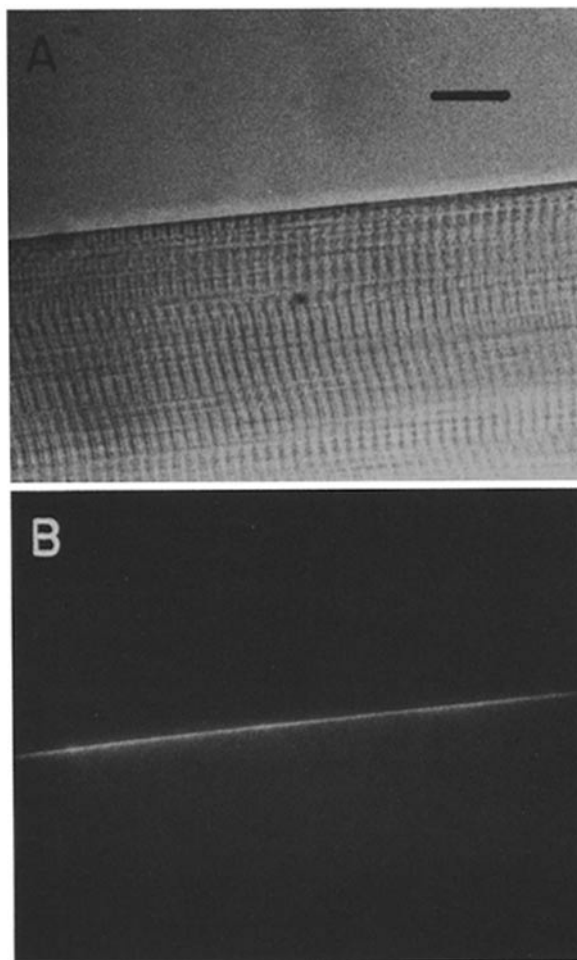

FIGURE 3.   Two light micrographs compare the appearance of a single muscle fiber stained with FITC-WGA under bright-field (A) and epi-illumination for fluorescence (B). The plane of focus is at the level of the center of the fiber.

experiment also shows that repeated fluorescence measurements cause negligible photobleaching of the chromophore.

Mobility of Lectin Receptors in the Plane of the Sarcolemma

The mobility of WGA receptors can be investigated by FRAP. In this method, the surface of a cell is first labeled with a fluorescent ligand, the fluorophores in a small area of labeled membrane are then bleached, and the fluorescence of

that area is monitored thereafter to test whether it recovered. Fig. 4 *C* shows the area of membrane in Fig. 4*B*, photographed almost immediately after an 80-s illumination with a spot of intense 390–490-nm light. Where the light fell, little fluorescence remained, and the outlines of the bleached region are sharply
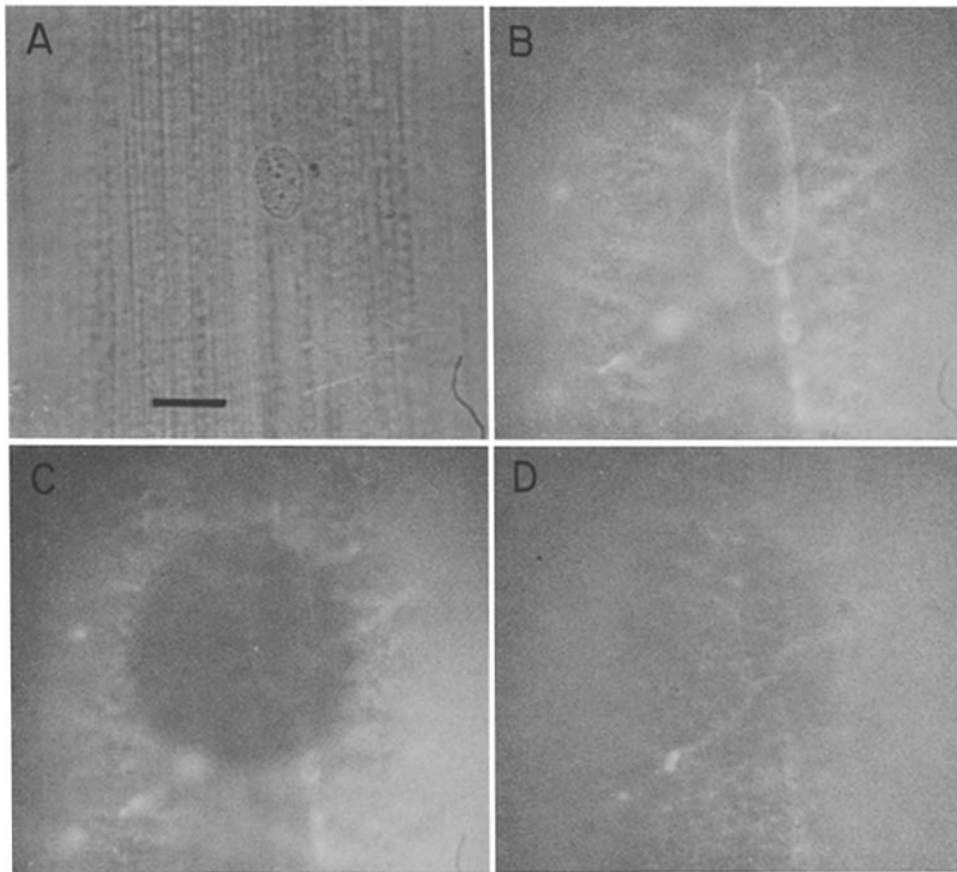

FIGURE 4.   Surface view of an FITC-WGA–stained single muscle fiber. The fiber was lightly compressed between two coverslips to create a flat region of sarcolemma in the plane of the picture, and the microscope was focused onto that surface. Panels *A* (bright-field illumination) and *B–D* (fluorescence optics) are all from the same area of the fiber, and were photographed in the sequence shown. *B* is before, *C* is 1.5 min after, and *D* is 36.5 min after bleaching the sarcolemma with a 31-μm-diam spot of intense blue light. The background brightness of the last two fluorescence panels was adjusted during printing to compensate for slight bleaching of the entire field, which occurred during photography. Calibration bar, 10 μm.

defined. The fluorescence in the bleached area had largely recovered 36.5 min later (Fig. 4*D*); only a faint outline of the bleached spot remained. Following other investigators, who have performed similar experiments on other types of cells, we interpret the recovery of fluorescence as being due to fresh WGA receptors that, carrying along their unbleached fluorophores, migrate into the

bleached area by diffusion within the cell membrane. This interpretation is the simplest, since the bath contained no fluorescent material and the material bound elsewhere on the muscle did not dissociate within the times explored here (see above). Also consistent with this interpretation was the appearance of the small cell, which was situated entirely within the bleached area and lost its fluorescence completely (Fig. 4C). The fluorescent outline of this cell did not reappear (Fig. 4D). Evidently the recovery of fluorescence observed here depended on continuity with a large reservoir of unbleached membrane.

To determine the time course of recovery in this type of experiment, the local concentration of fluorophore in a small area of sarcolemma was periodically assayed by flashing images of a small circular spot of exciting light onto the sarcolemma and measuring the resulting fluorescence with a photomultiplier (see Methods). Fig. 5A shows an experiment on a fiber labeled with FITC-WGA. The ordinate shows the normalized fluorescence from a 7.2-μm-diam spot on the sarcolemma. Immediately before $t = 0$, fluorescence measurements were suspended while the exciting beam was intensified 10-fold so that, during 15-s continuous illumination, much of the fluorophore in the spot was bleached. Then periodic sampling of fluorescence with dim excitation light was resumed. It can be seen that fluorescence from the spot was diminished strongly by the intense light, but recovered partially during the following 50 min. As before, we attribute the recovery to lateral diffusion of WGA receptors that carry unbleached fluorophore.

The continuous curves in Fig. 5 are given by

$$F = F_0 + m(1 - F_0)\left[1 - 4 \sum_{n=1}^{\infty} \frac{\exp(-D\alpha_n^2 t/a^2)}{\alpha_n^2}\right], \tag{1}$$

which describes radial diffusion into a disk. The expression gives the average concentration of the diffusing substance inside the disk (e.g., Crank, 1970, Eqs. 5.14 and 5.23) after this concentration has been uniformly reduced to a fractional value, F_0. α_n are the roots of $J_0(x) = 0$, $J_0(x)$ being the Bessel function of zero order and the first kind. D is the radial diffusion coefficient and a is the radius of the illuminated (and bleached) spot. It is assumed that not all of the fluorophore is free to diffuse, and that the freely diffusible fraction is m. In Fig. 5A, where F_0 is measured as 0.35, the best least-squares fit is obtained with $D = 5.6 \times 10^{-11}$ cm^2/s and $m = 0.50$. The curve is seen to describe the data well.

In 14 similar experiments on 11 fibers, average values were $D = 6.4 \times 10^{-11}$ cm^2/s ($\pm 0.8 \times 10^{-11}$ cm^2/s [SEM]) and $m = 0.53 \pm 0.02$. The magnitude of the mobile fraction of sarcolemmal WGA receptors may be somewhat larger than the value of m, since any WGA receptors in the basement membrane and adhering connective tissue strands would appear immobile. When FRAP measurements were performed twice on the same spot on a muscle fiber, the diffusion coefficients obtained were identical within experimental error, with the ratio of the first over the second measurement being $D_1/D_2 = 0.84 \pm 0.13$ SEM ($n = 5$). However, the mobile fraction in the second experiment was always increased, because the immobile fraction does not recover its fluorescence. We conclude that the excitation light used to bleach the fluorophore did not significantly affect the mobility of WGA receptors.

Fig. 5*B* illustrates a FRAP experiment on a fiber stained with FITC-sConA. This dimeric lectin (52,000 mol wt) binds preferentially to α-D-mannose and α-D-glucose residues, and the receptors for this lectin are thought to be distinct from those for WGA (Ozanne and Sambrook, 1971; Janson and Burger, 1973; Janson et al., 1973). No significant recovery of fluorescence was observed, which indicates that only a vanishingly small fraction of the sConA receptors are measurably mobile. The finding could be explained if the label bound more
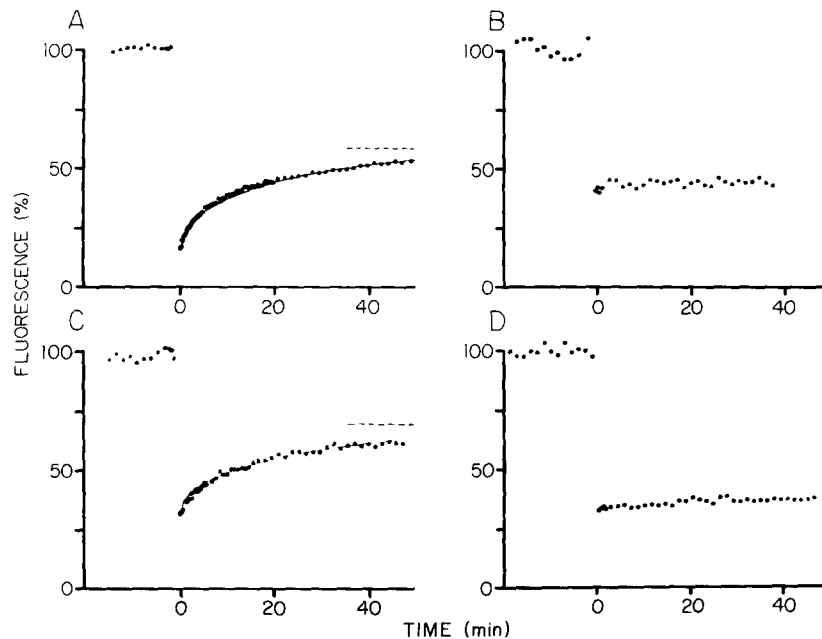

FIGURE 5. Fluorescence recorded from small spots of sarcolemma on four muscle fibers labeled with FITC-conjugated lectins. Each point is the average of three measurements. At $t = 0$, fluorescence was diminished by continuous illumination (6–20 s) with the 10–100-times-intensified excitation beam. Fluorescence is seen to recover when the label was FITC-WGA (*A* and *C*) but not when it was FITC-sConA (*B* and *D*). *A* and *B* were in Ca-free relaxing solution (see Methods); *C* and *D* were in Ringer fluid; both solutions were lectin-free. The spot size was 7.2 μm; all measurements were made with a 50× Leitz water immersion objective. Continuous curves are given by Eq. 1 with the parameters $F_0 = 0.15$, $D = 0.56 \times 10^{-10}$ cm²/s, $m = 0.50$ (*A*), and $F_0 = 0.32$, $D = 0.44 \times 10^{-10}$ cm²/s, $m = 0.44$ (*C*). The dashed lines indicate the predicted recovery at infinite time. Experiments 0024 (*A*), 0070 (*B*), 0059 (*C*), and 0055 (*D*).

heavily to the basement membrane than to cell membrane receptors, so that fluorescence from the rigid basement membrane would mask that from mobile receptors in the sarcolemma. This explanation would be consistent with the composition of the major basement membrane proteins. For instance, collagen has a high content of glucose residues, and fibronectin is rich in mannose, but neither protein contains comparable amounts of WGA binding residues such as sialic acid (Kefalides, 1973; Carter and Hakomori, 1971). Fibronectin is known

to bind considerable amounts of concanavalin A (Gahmberg and Hakomori, 1975) and the same appears to be true for the whole basement membrane of skeletal muscle (Wakayama et al., 1980).

Most of our FRAP experiments were done in a Ca-free, K-rich solution (see Methods) that depolarized the muscle sufficiently to make it mechanically refractory. This was done because even the slightest movement during the ~1-h-long experiment produced large errors by diminishing the coincidence between the bleached area and that from which fluorescence was assayed. Nevertheless, a few successful experiments were also carried out in Ringer fluid (Fig. 5, *C* and *D*) and gave similar results. About half of the WGA receptors, but virtually none of the sConA receptors, were measurably mobile.

Destruction of Na and K Channels by UV Irradiation

Our method of studying the mobility of ion channels relies on the localized photodestruction of channels by UV light. Fig. 6, *A–C*, shows membrane currents recorded through a patch pipette (see Methods) during step depolarizations of 80 (*A*), 140 (*B*), and 130 (*C*) mV. During the 80-mV pulse, a transient inward current (I_{Na}) through voltage-activated, tetrodotoxin-sensitive Na channels predominated. During the 130- or 140-mV pulses, I_{Na} was smaller and followed by a more slowly developing outward current (I_K), which, on the basis of previous work (Adrian et al., 1970; Stanfield, 1970) flows through voltage-activated K channels that are blocked by tetraethylammonium (not shown) and are often referred to as delayed rectifier channels. Currents through Na channels cause the upstroke of the action potential, while delayed rectifier channels contribute to repolarization.

Each of the panels in Fig. 6 shows two traces. The trace with the deflections of larger amplitude was recorded before, and the other trace after a period of through-the-pipette irradiation with UV light (289 nm in Fig. 6). The traces show that UV light caused a loss of current through both Na and K channels. When irradiation was continued for long enough, these currents were lost entirely (Fig. 6*C*).

In Fig. 6, *D* and *E*, I_K and peak I_{Na} are plotted against time. Both I_{Na} and I_K begin to decline exponentially as soon as irradiation starts ($t = 0$). I_{Na} declined more rapidly than I_K; evidently Na channels are more sensitive than K channels to UV light. Similar results were previously obtained by Oxford and Pooler (1975) on lobster axons, and by Fox and Stämpfli (1971) and Fox (1974) for Na channels in myelinated nerve. These authors found that the effects of UV light are irreversible, and that, at least for I_{Na}, the surviving channels remain normal in kinetics and voltage dependence. These results, along with the exponential decline of I_{Na} and I_K, have led to the view that Na and K channels are destroyed by UV light in a one-hit, one-photon event.

The sensitivity to UV can be measured as the rate constant of decline divided by the power density of the light reaching the membrane beneath the pipette. The power of the light leaving the pipette was measured after each experiment by passing the pipette tip through a pinhole covering the photosensitive surface of a UV-sensitive photodiode. To obtain the power density, the value obtained was divided by the area of the pipette tip orifice, measured from photographs as

in Fig. 2. As an approximation, this seems justified because light is known to leave the pipette as a well-defined beam of the same diameter as the pipette tip orifice (Stühmer and Almers, 1982). Effects of nonuniform illumination of the patch were neglected.
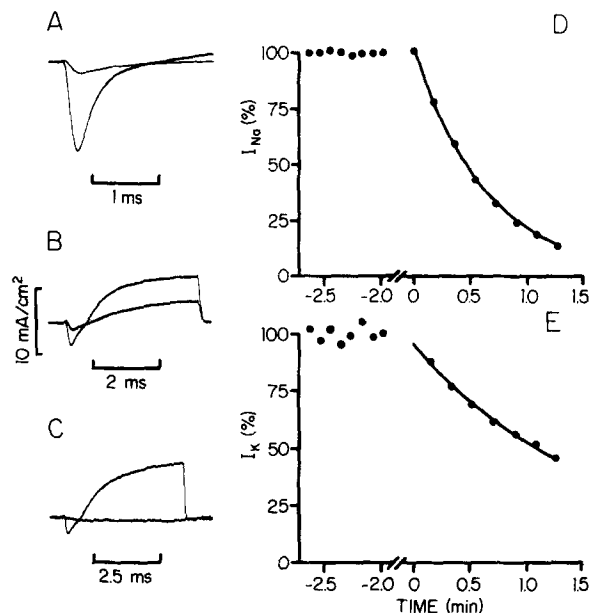

FIGURE 6. Photodestruction of Na and K channels by UV light. (Left) Current traces during steps of 80 (A), 140 (B), and 130 (C) mV amplitude, recorded before (large deflections) and after (smaller deflections) a period of continuous irradiation with 289 (A, B) or 280 (C) nm UV light. UV light reached the membrane by being piped through the patch pipette (see Methods). A and B are from a patch formed by a pipette with a 30-μm tip diameter. The intensity of UV light, divided by the area of the pipette tip orifice, was 7.9 mW/cm^2; the period of irradiation was 80 s. Experiment PU24. C is from another experiment (KMB5) with a 12-μm pipette; the essentially flat trace was recorded after 3 min of irradiation. (Right) Absolute values of peak I_{Na} (D) and I_K (E) plotted against time. I_{Na} and I_K were measured during alternating pulses of 80 and 140 mV amplitude, respectively. Peak I_{Na} was measured as in Stühmer and Almers (1982) with respect to the baseline before depolarization; I_K was measured at the end of the pulse as the amplitude of the current jump at the moment of repolarization. Irradiation started at $t = 0$. The continuous curves are the best least-squares fit of exponential functions that decline to zero; their time constants are 36 (D) and 102 (E) s. Same experiment as in A and B.

Fig. 7 shows an action spectrum, plotting the sensitivity to UV light (S) against wavelength. S is the reciprocal of the radiation dose required for an e-fold reduction of I_{Na} (circles) and I_K (squares). The wavelengths chosen were the mercury lines provided by the arc lamp. Both Na and K channels are most sensitive at 280–289 nm, as if UV light attacked one or more aromatic amino

acids forming part of the channel protein. At 289 nm, 0.40 J/cm^2 was sufficient to reduce the number of functional Na channels e-fold; for K channels, 0.94 J/cm^2 was required. In this series of experiments, K channels were nearly three times less sensitive than Na channels. However, the sensitivity ratio was variable; in a later series (see Fig. 12), Na and K channels were much more similar in their sensitivity to UV light. The reasons for this variability are not understood.
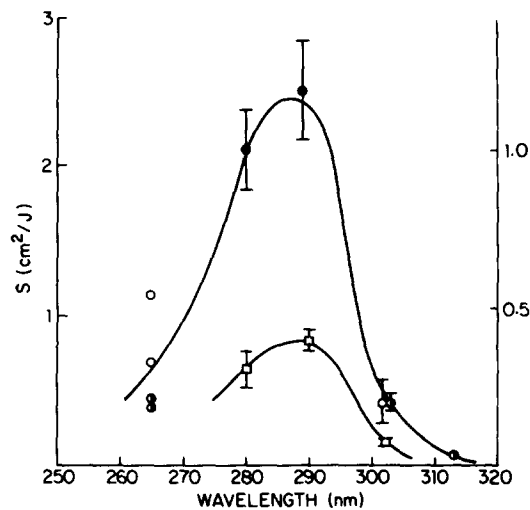

FIGURE 7. Action spectrum for the destruction of Na channels (circles) and K channels (squares) by UV light. The solid circles at 280 and 289 nm were obtained as in Fig. 6, and the left-hand ordinate applies to them. They represent the reciprocal of the radiation dose required for an e-fold reduction of I_{Na} (circles) and I_K (squares). S is defined by $S = \beta/H$, where H is the UV light intensity at the pipette tip (in watts per square centimeter) and β is the initial rate constant for the decline of I_{Na}, calculated as the reciprocal of time constants as obtained in Fig. 6, D and E, on the assumption that current declines exponentially to zero. For the right-hand ordinate, the mean sensitivities S for I_{Na} at 280 and 289 nm were assigned the values 1.0 and 1.19, respectively. All other open symbols were normalized relative to measurements of the initial rate constant of I_{Na} decline at either 280 or 289 nm, made on the same patch (squares at 280 and 289 nm) or with the same pipette on the same fiber. The value of H was determined for each pipette and at all wavelengths of interest, generally both before and after each series of electrophysiologic measurements. Patch diameters in these experiments were 20–30 μm. Half-filled symbols represent values obtained with the vaseline-gap technique. They were calculated from the initial rate constant of I_{Na} decline, and are given relative to measurements on the same fiber carried out at 280 nm.

We performed similar measurements of I_{Na} also with the vaseline-gap technique (Hille and Campbell, 1976; Almers et al., 1982). A reflecting objective was used to focus UV onto the fiber, and the section of the fiber from which we recorded current, i.e., the A-pool, was covered with a small piece of quartz coverslip to exclude the vaseline film that normally forms at the air-water interface. The

decline of I_{Na} in these experiments was only poorly described by an exponential, presumably because muscle fibers strongly absorb UV, so that irradiation reaches only the half of the fiber surface facing the UV source. If an apparent value of S is calculated from the initial rate constant of decline of I_{Na}, the average value is $S = 1.08 \pm 0.04$ cm^2/J ($n = 4$, $\pm$ SEM), roughly half that observed with the loose-patch method. However, in calculating rate constants, it would probably be more reasonable to refer the initial rate of decline to half the current observed, since only half the membrane from which we collect current is likely to be reached by UV. If this is done, the value of S doubles, and is in good agreement with the loose-patch measurements.

From results obtained with the vaseline-gap technique on myelinated nerve by Fox and Stämpfli (1971, their Fig. 1), one can calculate $S = 0.7$ cm^2/J for I_{Na} in that tissue. These authors reported also that K channels of myelinated nerve are not measurably sensitive to UV. In lobster axons, K channels were 10 times less sensitive to UV than Na channels (Oxford and Pooler, 1975). The lesser sensitivity of K channels to UV seems to be a general finding.

Mobility of Na and K Channels

Since the patch pipette allows both local recording and local irradiation, one can use it to investigate the mobility of ion channels (Stühmer and Almers, 1982). If channels are mobile, current from an irradiated patch should recover as healthy channels diffuse into the patch from the surrounding membrane. Fig. 8 (left) shows signal-averaged records of I_K and I_{Na} (A) and of I_{Na} alone (C), all obtained from the same patch. Each panel shows three traces superimposed. Trace 1 was recorded before, trace 2 immediately after, and trace 3 ~16 min after the end of the irradiation period. In Fig. 8A, trace 3 is slightly larger than trace 2, which indicates a slight recovery of I_K after irradiation. The difference between the two traces is shown at a 10-fold-higher gain in Fig. 8B (noisy trace), with a scaled version of trace 1 superimposed. The difference trace is seen to have a component that is kinetically similar to the late outward current, i.e., to I_K, but no inward component that resembles I_{Na}. The difference between traces 2 and 3 in Fig. 8C is shown in Fig. 8D. Once again, it has an outward but no inward component. It can be concluded that after irradiation, there is a slight recovery of I_K, but none of I_{Na}.

When I_K and peak I_{Na} from this experiment were plotted against time (Fig. 9, A and C), I_{Na} did not show recovery after irradiation, which confirms that Na channels are not measurably mobile by this technique (Stühmer and Almers, 1982). There was, however, a slight recovery of I_K, which indicates either that the effects of UV on K channels are partially reversible, or that a small number of K channels entered the irradiated patch by diffusion within the plane of the membrane.

The experiment in Fig. 9B was similar to that of Fig. 9A, but was carried out with a pipette of large tip diameter. Although measurements at late times (not included) showed that some recovery of I_K ultimately did take place, it is clear that any such recovery in Fig. 9B was considerably slower than in C. A depend-
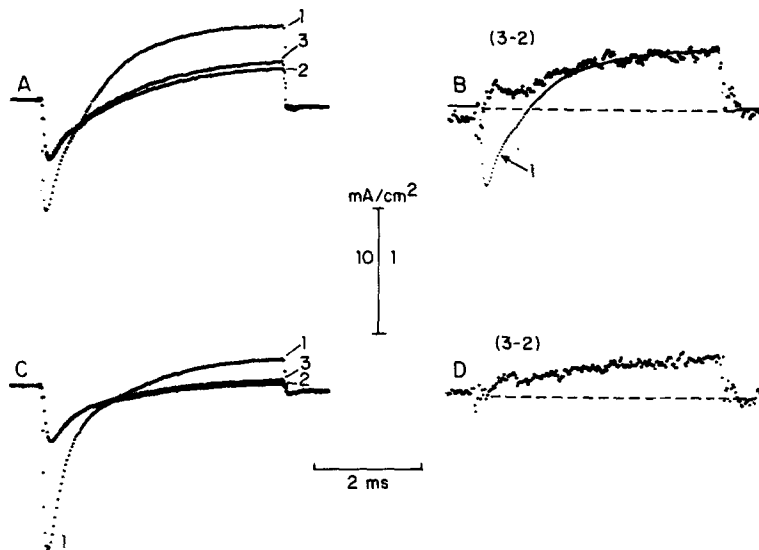
FIGURE 8. Membrane currents during 130-mV (*A* and *B*) and 90-mV (*C* and *D*) depolarizations. Panels *A* and *C* show three traces each; each trace is the average of six measurements. Trace 1 is from measurements obtained between 0 and 3.5 min before, trace 2 from measurements between 1 and 4 min after, and trace 3 from measurements taken between 14 and 17 min (*A*) or 16 and 18 min (*C*) after irradiation with 289-nm UV light. Panel *B* shows the difference between traces 3 and 2 of panel *A*, and panel *D* shows the differences between traces 3 and 2 of panel *C*. For comparison, a scaled version of trace 1 in *A* (labeled 1) is superimposed onto the difference trace in *B*. In this figure, it was important to reduce noise, most of which comes from the signal that is subtracted from the measured current to correct for stray capacity and leakage under the seal (Almers et al., 1983). To eliminate this source of noise, the leakage-capacity signal was divided into the following six sections: (1) before depolarization, (2) 0–0.25 and (3) 0.25–1.5 ms after depolarization, (4) between 1.5 ms after depolarization and repolarization, (5) 0–0.25 ms after repolarization, and (6) from 0.25 ms after repolarization until the end of the trace. Sections 1, 3, 4, and 6 were replaced with least-squares fits of polynomials of order 0, 3, 2, and 3, respectively. The resulting smooth curves were used instead of the raw signal for leakage and capacity subtraction. Immediately after a potential step (sections 2 and 5), the current changed too rapidly to be fitted satisfactorily; during that time, the raw signal was used for subtraction. The difference between the raw signal and its replacement was routinely displayed on the oscilloscope and showed no systematic deviation from zero over the entire length of the trace. Fiber KMB3; pipette diameter, 11 μm.

ence on pipette tip diameter is not expected if recovery is simply due to reversion from a hypothetical, UV-induced inactive state. Recovery by lateral diffusion, on the other hand, is expected to depend strongly on pipette tip diameter, being slowed fourfold when the diameter is doubled. Hence, our results favor the view that the recovery in Fig. 9*A* was due to diffusion of fresh K channels into the irradiated patch.

The recovery of I_K in Figs. 8 and 9 was only slight, but it was observed consistently. In Fig. 10, five experiments including those in Fig. 9, A and C, were combined by signal-averaging. To allow for differences in pipette diameter, the time axis in each experiment was normalized to correspond to a 10-μm tip diameter; this was done by multiplying the abscissa by $(10\ \mu\text{m/diam})^2$. To allow
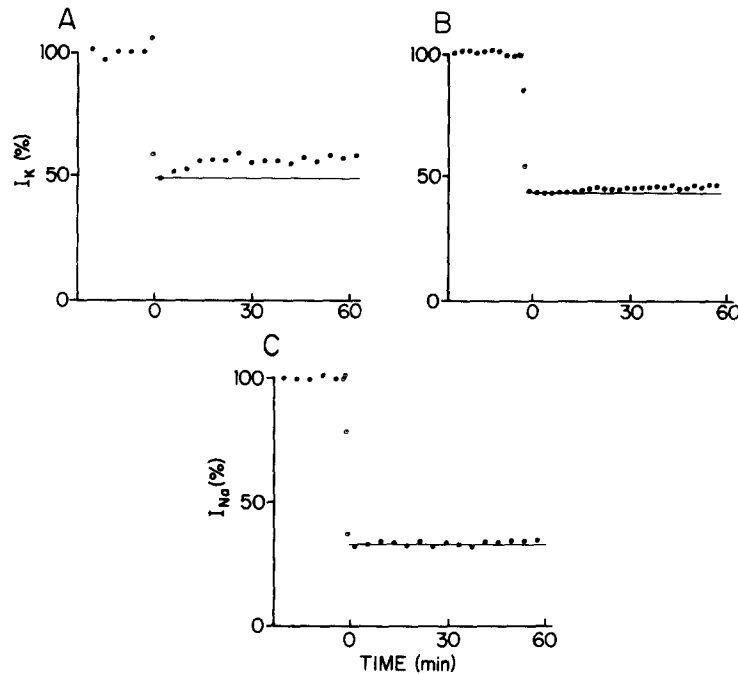

FIGURE 9. Time course of I_K (A and B) and I_{Na} (C) after through-the-pipette irradiation with 289-nm UV light. From Fig. 7, the energy density can be calculated as having been between 0.43 and 0.88 J/cm^2, since at $t = 0$, I_{Na} was reduced to 34% (C) and I_K to 48% (A) or 39% (C). A and C are from an experiment where I_{Na} and I_K were measured as in Fig. 6, D and E, during alternating pulses of 90 and 130 mV amplitude, respectively. Each point is the average of eight measurements except immediately before and during the irradiation period, where single measurements are plotted. At the end of the experiment, the pipette was moved to two other locations, spaced 20 μm apart along the fiber axis; K currents recorded there were at 110 and 92%, and Na currents were at 94 and 70% of the mean value recorded before irradiation. Fiber KMB3; pipette diameter, 11 μm; same experiment as in Fig. 8. B was obtained from another fiber (KM04) with a larger (20 μm diam) pipette tip. The horizontal lines indicate the current immediately after irradiation.

for the fact that I_K was reduced to slightly different degrees in different experiments, plots as in Fig. 9, A and C, were treated as follows. First, a constant was added to all ordinates to make I_K immediately after irradiation equal to half the average current before irradiation. Then the ordinates were normalized with respect to the mean I_K before irradiation. Finally, all five experiments were superimposed, and adjacent groups of 30 points were averaged. Fig. 10 clearly shows that a small fraction of I_K recovered after irradiation.

For quantitative analysis, we followed previous practice and assumed that UV emerges from the pipette tip as a beam of Gaussian intensity profile, with the intensity decreasing by a factor of e^2 within the pipette tip radius a, i.e., within 5 μm for Fig. 10. The efficiency of current collection was assumed to vary with the same profile. In that case, recovery of current should be given by (Axelrod et al., 1976a):

$$F = F_0(1 - m) + m \sum_{n=1}^{\infty} \frac{(-K)^n}{n![1 + n(1 + 8Dt/a^2)]}, \tag{2}$$

where K is calculated from

$$F_0 = (1 - e^{-K})/K \tag{3}$$

and has the value 1.59 if $F_0 = 0.5$. The dashed curve was drawn with $m = 1$ and $D = 5 \times 10^{-12}$ cm^2/s, and the continuous curve with $m = 0.25$ and $D = 5 \times 10^{-11}$
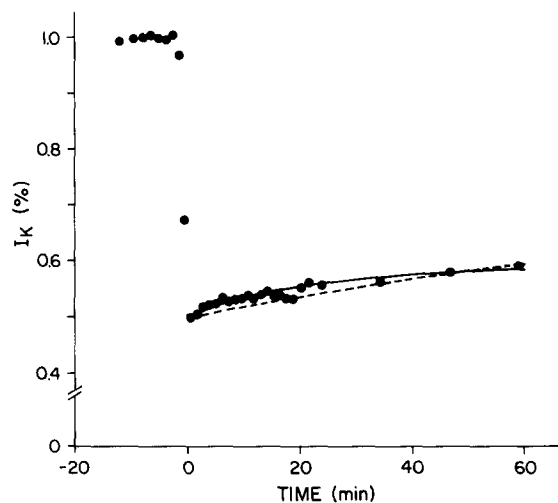

FIGURE 10. Recovery of K current after UV irradiation; average results from five experiments as in Fig. 9, A and C. Experiment references, pipette diameters, and fractional current after irradiation are as follows: KMB3, 11 μm, 0.43; KM68, 13 μm, 0.65; KM06, 17 μm, 0.42; KM05, 18 μm, 0.53; KM04, 20 μm, 0.47. The dashed and continuous curves were drawn by Eq. 2 with the parameters $D = 5 \times 10^{-12}$ cm^2/s, $m = 1$ (dashed), and $D = 5 \times 10^{-11}$ cm^2/s, $m = 0.25$ (continuous). The continuous curve provides the better fit.

cm^2/s. The continuous curve provides the better fit. Hence, we conclude that although most K channels are immobile, there is also a small fraction (25%) whose mobility is about equal to that of the WGA receptors in Fig. 5.

Lack of Effect of UV Irradiation on the Mobility of WGA Receptors

The failure of Na and K channels to diffuse readily into an UV-irradiated patch could be explained if the UV irradiation transformed the sarcolemma into a rigid structure into which membrane proteins could not diffuse. Fig. 11 tests this
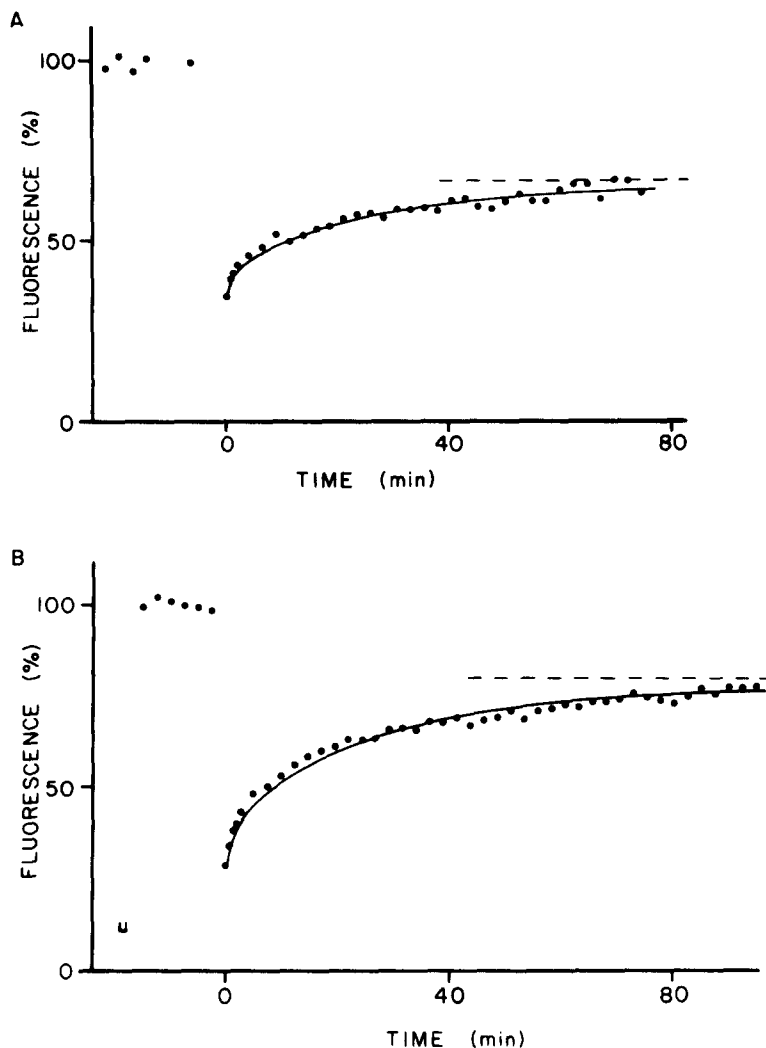
FIGURE 11. Effect of UV irradiation on the mobility of FITC-WGA receptors. (A) Experiment similar to that in Fig. 5A, except that a UV-transmitting reflecting objective was used, and the spot size was 5 μm. (B) As in A, except that the measurement was carried out after irradiation with 289-nm light. UV irradiation was carried out through the same light path that was used to excite fluorescence, except that all optical elements between the electronic shutter and the dichroic mirror were removed and replaced by a 289-nm bandpass interference filter. The UV intensity that arrived at the plane of the muscle fiber was measured before and after the experiment with a UV-sensitive photodiode (see Methods). From it and the irradiation time, we calculated an energy density of 1.56 J/cm² for this experiment. The continuous curves are given by Eq. 1 with the parameters $F_0 = 0.35$, $D = 2.5 \times 10^{-11}$ cm²/s, $m = 0.49$ (A, experiment 0088) and $F_0 = 0.27$, $D = 2.4 \times 10^{-11}$ cm²/s, $m = 0.72$ (B, experiment 0089). A and B were obtained on the same fiber.

possibility, and shows two FRAP experiments on an FITC-WGA–labeled fiber. The data in Fig. 11A were obtained as in Fig. 5A, and plot the recovery of fluorescence in a 5.0-μm-diam bleached spot against time. In Fig. 11B, a 5.0-μm-diam spot on the same fiber was first irradiated with 1.5 J/cm^2 of 289-nm light, and then the ability of WGA receptors to diffuse within that area was measured as in Fig. 11A. On the basis of Fig. 7, the energy density of UV deposited on the membrane would have been large enough to diminish the number of functional K channels four- to fivefold, more severely than in the experiments of Figs. 9 and 10. Even with this large dose of UV irradiation, however, fluorescence recovery indicated a diffusion coefficient for WGA receptors that was essentially identical to that measured on an unirradiated patch. Measurements after irradiation with 280- or 289-nm light at an average dose of 1.29 J/cm^2 (range, 0.67–1.56 J/cm^2) were made on a total of four fibers. The average post-irradiation diffusion coefficient was 2.6×10^{-11} cm^2/s ($\pm 0.5 \times 10^{-11}$ cm^2/s) and the average mobile fraction 66.2 ± 6.2%; values are given ± SEM. These values are nearly identical to others obtained without irradiation on fibers from the same muscles ($D = 2.8 \times \pm 0.5 \times 10^{-11}$ cm^2/s; $m = 58.6 \pm 9.4\%$; $n = 5$). We conclude that the apparent lack of Na and K channel mobility is not due to the UV irradiation.

Size of the Irradiated Area

The analysis of Fig. 10 assumes that the irradiation destroys Na and K channels only in a strictly localized area. While this assumption is supported by the finding that UV light supplied to the back end of the pipette leaves the tip as a sharply defined beam of the same diameter as the pipette tip orifice (Stühmer and Almers, 1982), it seemed desirable to map the amount of photodestruction directly in nearby and overlapping patches by recording current as a function of position. In achieving this, we faced two difficulties. First, the distribution of Na and K channels is known to be nonuniform even before irradiation (Almers et al., 1983). Second, it seemed possible that repeated attempts to make seals on overlapping membrane areas might cause changes in current unrelated to UV irradiation, possibly through membrane deformation. Recordings were therefore made from only two locations on each fiber, and the results from many fibers were averaged.

A first series of experiments served to test for changes in current attributable to forming a patch. The pipette was advanced until a seal resistance of 0.4 MΩ was attained, and Na currents were measured with a 90-mV step (I_{Na1}) and K currents with a 130-mV step (I_{K1}). The pipette was then withdrawn and a new patch with a 0.4-MΩ seal was made, either at the same location or at a distance of up to 50 μm along the longitudinal axis of the fiber. The currents recorded after the second approach, I_{Na2} and I_{K2}, were divided by I_{Na1} and I_{K1}, respectively, and plotted against patch separation. Patch separation is defined as the center-to-center distance between the two patches. Fig. 12 (solid symbols) shows the results of 108 such experiments. For I_{Na}, the average ratio is seen to be independent of patch separation and was not significantly different from unity (Fig. 12A). I_K, however, was slightly reduced when the second patch overlapped the

first. Fig. 12*B* suggests that I_K was diminished locally by ~10% when a 0.4-MΩ seal was made with a pipette of 14 μm tip diameter.

To map the effects of UV irradiation on I_K and I_{Na}, we used the same experimental protocol as above, except that after I_{Na1} and I_{K1} had been measured, UV light was applied through the pipette until I_{Na} fell to half its initial value. The pipette was then withdrawn and re-advanced, either at the same or another location. I_{Na} and I_K were recorded once again, normalized as before, and plotted against patch separation. Fig. 12 (open symbols) shows the result from 90 experiments of this kind. As expected, currents close to the irradiation site were
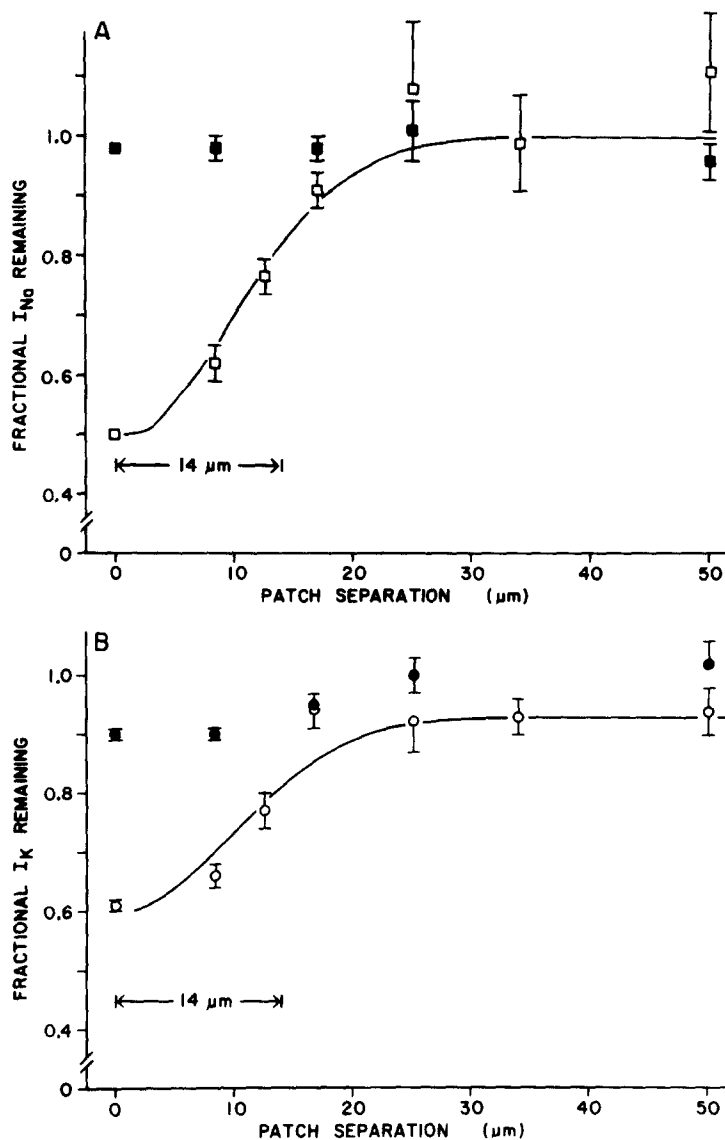
strongly reduced. However, the effect of UV rapidly diminished with increasing distance and, for Na channels, vanished altogether when the patch separation was >25 μm (Fig. 12A). With K channels, a small (~7%) reduction of I_K was seen even at the largest separations (Fig. 12B) as if, in addition to acting locally, UV also had a more diffuse effect that spread uniformly over distances at least as large as 50 μm. The significance and mechanism of the diffuse UV effect on K channels are not understood.

The smooth curves in Fig. 12 show, as a function of patch separation, the decrement in current expected if the overlap of two nearby patches is taken into account. As in Fig. 10, we assumed UV light arriving at the membrane to have a Gaussian intensity profile that is maximal at the center of the patch, decreases e^2-fold within one pipette radius, and continues to decline to zero outside the pipette. The amount of channel photodestruction at each point in the membrane was assumed to be proportional to the local UV intensity. For I_K, we assumed a spatially uniform 7% reduction in addition to the local effect of UV light. The efficiency of current collection was assumed to have the same Gaussian profile as the UV intensity. The curves are seen to provide a good fit to the data. Hence, these data support the view that the destruction of Na and K channels by UV irradiation is confined almost entirely to the membrane beneath the pipette tip, and can be described by the Gaussian profiles assumed in Fig. 9.

Variability of Na and K Current Densities Along the Fiber

Fig. 12 shows that if no irradiation was applied, currents did not vary systematically with position on the fiber. However, individual pairs of measurements on the same fiber showed a substantial variation that increased with distance between the two patches and most probably reflects a patchy distribution of Na and K channels over the sarcolemma. Fig. 13 plots, against patch separation, the average fractional difference in current recorded at the two locations. For Na currents, the difference is calculated by:

$$\Delta I_{Na} = 2[I_{Na1} - I_{Na2}]/[I_{Na1} + I_{Na2}], \tag{4}$$

FIGURE 12. (*opposite*) Spatial profiles of average Na and K channel densities before (solid symbols) and after (open symbols) photodestruction of Na and K channels by UV irradiation through the pipette. Smooth curves are theoretical current profiles generated for a 14-μm pipette, assuming a Gaussian profile of UV irradiation and current measurement across the pipette tip (for further explanation, see text). The data were obtained from 10 sartorius muscles. Each point is the mean of between 10 and 30 paired patches. To avoid bias, all accessible fibers in a muscle were used, and results were rejected only if the fiber showed evidence of being depolarized or if the current traces were suggestive of large rim currents (see Methods). The tip diameters of pipettes used for UV irradiation were 14 μm when patch separations were <17 μm, and 15 μm for some measurements with larger separations. In experiments without irradiation, smaller pipettes were also used, and we routinely retained the first patch for ~1 min after measurements were complete, and only then withdrew the pipette in order to approach the second patch. This waiting time was about equal to the usual time of irradiation.

where the brackets denote absolute values. For K currents, the situation is complicated by the fact that forming a patch in itself reduces I_K by ~10%. To allow for this systematic variation, one can calculate the difference ΔI_K by

$$\Delta I_K = 2[I_{K1} - rI_{K2}]/[I_{K1} + rI_{K2}], \tag{5}$$

where r, a function of patch separation, is the average value of I_{K1}/I_{K2} as obtained from Fig. 12B (circles). Eq. 5 was used for I_K instead of Eq. 4 for patch separations of <20 μm.

The average difference in current recorded when the pipette was withdrawn and repositioned over the same patch (0 μm separation) was ~5% for I_K and 3% for I_{Na}. The difference in current (and, presumably, channel) density increases as the area of overlap decreases, and reaches values of 13 and 16%, respectively,
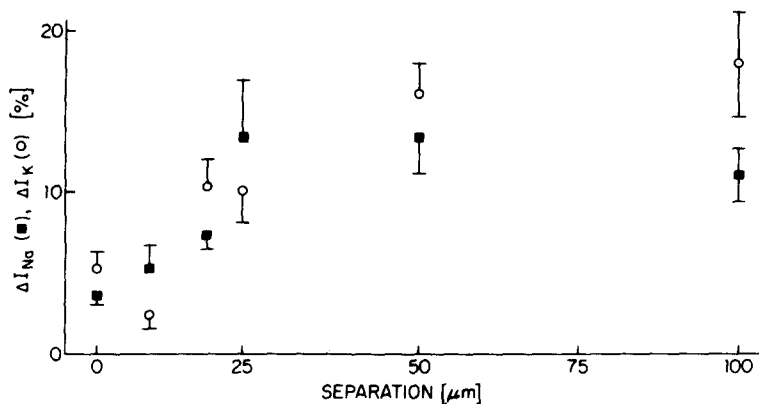

FIGURE 13. Mean fractional differences between currents recorded from two different patches on a fiber (see Eq. 4) as a function of patch separation. The data are the same as in Fig. 12 (solid circles), except for the points at 100 μm patch separation, which represent the mean from 16 fibers. For I_K, Eq. 5 was used instead of Eq. 4 when the patch separation was <20 μm.

at large patch separations. For I_{Na}, the maximal variation was attained at a patch separation of 25 μm, which indicates that the local densities of functional Na channels are spatially correlated over a distance not much larger than a patch diameter. For K channels, spatial correlation may extend over somewhat larger distances. The largest variation of I_{Na} found on a single fiber was $I_{Na2}/I_{Na1} = 2.1$, which corresponds to $\Delta I_{Na} = 71\%$. The largest value of I_{K2}/I_{K1} was 1.5, which corresponds to $\Delta I_K = 40\%$.

It might be argued that the variations reflect nothing more than differences in surface topography, which caused the pipette to collect from different amounts of sarcolemma at the two locations. This explanation requires that Na and K current densities vary proportionally among patches on the same fiber. However, there was no correlation between the ratios I_{Na2}/I_{Na1} and I_{K2}/I_{K1} (correlation coefficient = -0.06, $n = 65$; pooled data from paired patches separated by ≥ 25 μm). Thus, Na and K current densities appear to vary independently.

There is a larger variation in current densities recorded from different fibers than from patches on the same fiber. The range in this sample of 248 patches on 124 fibers was 5.2–27.0 mA/cm^2 for I_{Na} and 1.7–15.0 mA/cm^2 for I_K. The mean peak I_{Na} for all first patches was 12.0 ± 4.1 mA/cm^2 and the mean K current was 8.2 ± 3.0 mA/cm^2 (± sample standard deviation; $n = 124$).

DISCUSSION

This paper compares, in the same preparation, the mobilities of receptors for two divalent lectins, and of two voltage-dependent ion channels, Na and K channels. The main finding is that both ion channels are severely restricted in their mobility.

We confirm that Na channels are immobile, or have a mobility of $D = <10^{-12}$ cm^2/s (Stühmer and Almers, 1982). This is at least 1,000 times less than observed when an integral membrane protein with the molecular weight of the Na channel is released from cytoskeletal constraints and becomes freely mobile in the lipid bilayer (Tank et al., 1982). It is shown here that voltage-dependent K channels are also severely restricted in their mobility. Our data are best explained if most K channels (75%) are as immobile as Na channels, and if a minority (25%) have the same mobility as the average mobile WGA receptor.

Our measurements do not speak to the mechanism of immobilization. In fact, when stating that Na and most K channels are "immobile," we keep in mind that we tested for mobility over distances (several micrometers) that are large on a molecular scale. It is possible that both channels are free to rotate, or even that they have free translational mobility within small, "fenced-off" domains of submicron dimensions. Nonetheless, it is tempting to suggest that both Na and K channels may be immobilized by being anchored to cytoskeletal components, as seems to be the case for other membrane proteins.

In our method for measuring the mobility of ion channels, a glass micropipette was used for local recording of current from a small patch of cell membrane, and the amplitude of currents was used as an assay for the number of functional channels in the patch. Channels are locally destroyed by through-the-pipette irradiation with 289-nm UV light, and the re-invasion of the patch by functional channels was assayed by the contribution these channels make to the membrane current. It is shown here that both the photodestruction and current recording achieved with patch pipettes were strictly localized. Furthermore, UV at the required irradiation doses did not diminish the mobility of membrane proteins labeled with fluorescent WGA, and hence could not cause a general increase in the resistance of the cell membrane to diffusing particles. Finally, it should be noted that our experiments were done on fibers with an intact basement membrane. As discussed previously (Stühmer and Almers, 1982), the basement membrane prevents the tip of the micropipette from approaching the cell membrane to a distance of less than ~100 nm, so that the pipette is unlikely to provide a mechanical obstacle to diffusing membrane proteins. In any event, some channels in skeletal muscle sarcolemma do appear to invade the irradiated patch; hence, migration of ion channels beneath the pipette rim must be possible.

Our through-the-pipette method does not require the specific labeling of

membrane proteins. This is an important advantage, since labeled ligands to membrane proteins may influence mobility and may, in any case, not always be available. Instead, our method recognizes specific ion channels by the unique electrical signature shaped by their ion selectivity and response to potential changes. Although it has so far been applied only to Na and K channels, it may be applicable to other ion channels that can be opened and closed by potential changes, and that contain aromatic amino acids making them vulnerable to photodestruction by 289-nm light.

Mobility of WGA and sConA Receptors

WGA receptors are a heterogenous group that is made up mostly of various glycosylated integral membrane proteins, but includes also some glycolipids and peripheral membrane proteins of the basement membrane. Among the WGA-binding integral membrane proteins of the extrajunctional cell membrane are Na channels (Cohen and Barchi, 1981) and 1,4-dihydropyridine receptors (Curtis and Catterall, 1984). We find that half the WGA receptors on the muscle fiber surface are mobile and, although WGA is attached to them, have an average diffusion coefficient of 5×10^{-11} cm^2/s. As others have done, we view the mobile WGA receptors as representing a cross-section of mobile integral membrane proteins and interpret the single diffusion coefficient obtained as an average of values for several different integral membrane proteins. It is possible that the mobility of free WGA receptors would be higher, because the divalent WGA molecule may be bound to two receptors at once, and moreover may protrude into the viscous basement membrane and thereby retard the motion of the membrane receptor to which it is bound. The mobility obtained here is similar to that obtained in human embryo fibroblasts ($D = 8 \times 10^{-11}$ cm^2/s; $m = 0.8$; Jacobson et al., 1976). The mobile fraction in our experiments is smaller, but some of the WGA molecules are almost certainly bound to constituents of the basement membrane (Bonilla, E., and M. Moggio, personal communication) and others may be bound simultaneously to a receptor in the cell membrane and another in the basal lamina. In both cases, the WGA molecule would appear immobile, and hence our mobile fraction is an underestimate.

Unlike WGA receptors, the receptors for sConA, another divalent lectin, appear completely immobile. There is electron microscopic evidence that Con A binds so avidly to the basement membrane that binding to this essentially rigid structure predominates over that to the cell membrane (Wakayama et al., 1980). In our experiments, fluorescence from sConA bound to the basement membrane probably overwhelmed the signal from membrane receptors; hence, sConA receptors of the cell membrane may well appear mobile if they could be labeled selectively.

Significance for Skeletal Muscle

The example of WGA receptors shows that the sarcolemma of amphibian skeletal muscle contains both mobile and immobile membrane proteins. Clearly, Na and K channels are among the immobile membrane proteins. Both channels are known to be unevenly distributed over the cell membrane of amphibian skeletal

muscle. On the sarcolemma, they congregate in patches (Almers et al., 1983), and Na channels are present at particularly high density near the neuromuscular junction (Beam et al., 1985; Roberts and Almers, 1985). Furthermore, both channels populate the sarcolemma at higher density than the membranes of the transverse tubular system (Jaimovitch et al., 1976; Kirsch et al., 1977; Almers et al., 1982). This partial exclusion from the tubules is physiologically important, because the tubule membranes have a sizeable resistance in series and border on a space with restricted diffusional access. It is clearly necessary to have some Na channels in the tubules; otherwise, the action potential arriving in the center of the fiber would be too small for reliable contractile activation (Costantin, 1970; Bastian and Nakajima, 1974). With too many Na channels, on the other hand, the inevitably delayed activity in the transverse tubular system may become strong enough to re-excite the sarcolemma, which has become repolarized in the meantime. The fiber would give multiple action potentials in response to a single nerve impulse, a generally undesirable result. Having too many K channels in the tubules could result in excessive K accumulation there during an impulse, and hence in large afterdepolarizations. These in turn may result in repetitive discharges, as observed in goats afflicted with congenital myotonia (Adrian and Bryant, 1974). It seems likely that the distribution of Na and K channels between sarcolemma and tubules is carefully optimized. Immobilization of these channels helps explain how this distribution is maintained.

The mobility in the cell membrane has now been investigated for four ion transport proteins: acetylcholine receptors at the neuromuscular junction, the anion transport channel in red blood cells (band 3), and voltage-dependent Na and K channels. All four appear to be immobile, or at least severely restricted in their mobility. With band 3 and probably the ACh receptors, immobility is the result of anchorage to the cytoskeleton; the same may be true for Na and K channels. Since transport proteins are frequently concentrated in discrete locations on the cell surface (see Almers and Stirling, 1984, for review), it is tempting to suggest that transport proteins in cell membranes may be frequently or even generally immobile.

Irregular Density of Na and K Channels on the Sarcolemma

In the present work, the variations in I_{Na} and I_K encountered along the fiber are somewhat smaller than observed previously when moving the pipette across the fiber (Almers et al., 1983), but they are still too large to result from the random sampling of evenly distributed channels. This may be seen by considering average channel densities. The average value for peak I_{Na} at an estimated potential of -10 mV or 0 mV was 12 mA/cm^2, and that of maximal I_K at an estimated 30 mV was 8 mA/cm^2. Single channel currents i_{Na} and i_K in frog skeletal muscle have been measured by Standen et al. (1984) under experimental conditions similar to ours. From their work, one can estimate that $i_{Na} = 0.7$ pA at 0 mV, and $i_K = 1.3$ pA at $+20$ mV, and further that an average of 170 Na channels/μm^2 contribute to peak I_{Na}, and an average of 60 K channels/μm^2 to maximal I_K. If a pipette is placed over randomly distributed channels and collects current from an average number of n channels, the number of channels recorded from

in any actual experiment would vary with a standard deviation of $(n)^{-1/2}$. Since a typical 14-μm-diam pipette collects current from an average of ~26,000 Na and 9,000 K channels, we would expect a standard deviation of 0.6% for Na and 1% for K channels. In Fig. 13, substantially larger variations in I_{Na} and I_K were observed at all patch separations. Therefore, Fig. 13 confirms the earlier finding (Almers et al., 1983) that Na and K channels show a patchy distribution.

As in the previous work, there is no indication that current densities vary with the 2–3-μm periodicity that would be characteristic for structures associated with the sarcomere, e.g., the transverse tubular system. Even if such a periodicity existed, it probably would not have been resolved in Fig. 13. It is doubtful whether periodically varying K and Na current contributions from the transverse tubules would cause variations of the size observed here (Almers et al., 1983).

Surface Densities of Na Channels and Tetrodotoxin Receptors

The average peak I_{Na} density observed here can be compared with the density of tetrodotoxin binding sites (see also Hille and Campbell, 1976). This is of interest in view of results concerning 1,4-dihydropyridine binding sites, which are thought to represent Ca channels in skeletal muscle tubules. Apparently, only a few percent of all 1,4-dihydropyridine binding sites in skeletal muscle represent functional Ca channels that contribute to peak current in a voltage-clamp experiment (Schwartz et al., 1985). For Na channels, the situation is rather different. In myelinated nerve, analysis of Na current noise has shown that during a depolarization to −5 mV, ~60% of all functional Na channels may be open simultaneously and contribute to peak current (Sigworth, 1980). With an average of 170 Na channels/μm^2 contributing to peak inward current at that potential, frog sartorius muscle has an average of ~280 functional channels/μm^2 of sarcolemma that may be activated by, and pass current into, a patch pipette. There are 300–400 tetrodotoxin binding sites per square micrometer of sarcolemma (Almers and Levinson, 1975); 55% of them reside in the transverse tubules (Jaimovitch et al., 1976), where they are unlikely to contribute fully to peak current. Thus, all, or nearly all, tetrodotoxin binding sites are functional Na channels.

REFERENCES

Adrian, R. H., and S. H. Bryant. 1974. On the repetitive discharge in myotonic muscle fibers. Journal of Physiology. 240:505–515.

Adrian, R. H., W. K. Chandler, and A. L. Hodgkin. 1970. Voltage clamp experiments in striated muscle fibres. Journal of Physiology. 208:607–644.

Almers, W., R. Fink, and N. S. Shepherd. 1982. Lateral distribution of ionic channels in the cell membrane of skeletal muscle. In Diseases of the Motor Unit. D. L. Schotland, editor. John Wiley & Sons, New York. 349–366.

Almers, W., and S. R. Levinson. 1975. Tetrodotoxin binding to normal and depolarized frog muscle and the conductance of a single sodium channel. *Journal of Physiology*. 247:483–509.

Almers, W., P. R. Stanfield, and W. Stühmer. 1983. Lateral distribution of sodium and potassium channels in frog skeletal muscle: measurements with a patch-clamp technique. *Journal of Physiology*. 336:261–284.

Almers, W., and C. Stirling. 1984. Distribution of transport proteins over animal cell membranes. *Journal of Membrane Biology*. 77:169–186.

Axelrod, D., D. E. Koppel, J. Schlessinger, E. Elson, and W. W. Webb. 1976a. Mobility measurements by analysis of fluorescence photobleaching recovery kinetics. *Biophysical Journal*. 16:1055–1069.

Axelrod, D., P. Ravdin, D. E. Koppel, J. Schlessinger, W. W. Webb, E. L. Elson, and T. R. Podleski. 1976b. Lateral motion of fluorescently labeled acetylcholine receptors in membranes of developing muscle fibers. *Proceedings of the National Academy of Sciences*. 73:4594–4598.

Bastian, J., and S. Nakajima. 1974. Action potential in the transverse tubules and its role in the activation of skeletal muscle. *Journal of General Physiology*. 63:257–278.

Beam, K. G., J. H. Caldwell, and D. T. Campbell. 1985. Na channels in skeletal muscle concentrated near the neuromuscular junction. *Nature*. 313:588–590.

Bevan, S., and J. H. Steinbach. 1983. Denervation increases the degradation rate of acetylcholine receptors at end-plates *in vivo* and *in vitro*. *Journal of Physiology*. 336:159–177.

Campbell, D. T., and B. Hille. 1976. Kinetic and pharmacological properties of the sodium channel of frog skeletal muscle. *Journal of General Physiology*. 67:309–323.

Carter, W. G., and S. Hakomori. 1979. Isolation of galactoprotein A from hamster embryo fibroblasts and characterization of the carbohydrate unit. *Biochemistry*. 18:730–738.

Cohen, S. A., and R. L. Barchi. 1981. Glycoprotein characteristics of the sodium channel saxitoxin-binding component from mammalian sarcolemma. *Biochimica et Biophysica Acta*. 645:253–261.

Costantin, L. L. 1970. The role of sodium current in the radial spread of contraction in frog muscle fibers. *Journal of General Physiology*. 55:703–715.

Crank, J. 1970. The Mathematics of Diffusion. The Clarendon Press, Oxford, England. 65–66.

Curtis, B. M., and W. A. Catterall. 1984. Purification of the calcium antagonist receptor of the voltage-sensitive calcium channel from skeletal muscle transverse tubules. *Biochemistry*. 23:2113–2118.

Edidin, M., Y. Zagyanski, and T. J. Lardner. 1976. Measurement of membrane protein lateral diffusion in single cells. *Science*. 191:466–468.

Fertuck, H. C., and M. M. Salpeter. 1976. Quantitation of junctional and extrajunctional acetylcholine receptors by electron microscope autoradiography after ^{125}I-alpha-bungarotoxin binding at mouse neuromuscular junctions. *Journal of Cell Biology*. 69:144–158.

Fox, J. M. 1974. Selective blocking of the nodal sodium channels by ultraviolet radiation. I. Phenomenology of the radiation effect. *Pflügers Archiv European Journal of Pharmacology*. 351:287–301.

Fox, J. M., and R. Stämpfli. 1971. Modification of ionic membrane currents of Ranvier nodes by UV-radiation under voltage clamp conditions. *Experientia*. 27:1289–1290.

Frye, L. D., and M. Edidin. 1970. The rapid intermixing of cell surface antigens after formation of mouse-human heterokaryons. *Journal of Cell Science*. 7:319–335.

Gahmberg, C. G., and S. Hakomori. 1975. Sugar carbohydrates of hamster fibroblasts. II. *Journal of Biological Chemistry*. 250:2447–2451.

THE JOURNAL OF GENERAL PHYSIOLOGY · VOLUME 87 · 1986

Gulley, R. L., and T. S. Reese. 1981. Cytoskeletal organization at the postsynaptic complex. *Journal of Cell Biology.* 91:298–302.

Hille, B., and D. T. Campbell. 1976. An improved vaseline gap voltage clamp for skeletal muscle fibers. *Journal of General Physiology.* 67:265–293.

Hirokawa, N., and J. E. Heuser. 1982. Internal and external differentiations of the postsynaptic membrane at the neuromuscular junction. *Journal of Neurocytology.* 11:487–510.

Jacobson, K., Z. Derzko, E.-S. Wu, Y. Hou, and G. Poste. 1976. Measurement of the lateral mobility of cell surface components in single, living cells by fluorescence recovery after photobleaching. *Journal of Supramolecular Structure.* 5:565–576.

Jaimovitch, E., R. A. Venosa, P. Shrager, and P. Horowicz. 1976. Density and distribution of tetrodotoxin receptors in normal and detubulated frog sartorius muscle. *Journal of General Physiology.* 67:399–416.

Janson, V. K., and M. M. Burger. 1973. Isolation and characterization of agglutinin receptor sites. II. Isolation and partial purification of a surface membrane receptor for wheat germ agglutinin. *Biochimica et Biophysica Acta.* 291:127–135.

Janson, V. K., C. K. Sakamoto, and M. M. Burger. 1973. Isolation and characterization of agglutinin receptor sites. III. Studies of the interaction with other lectins. *Biochimica et Biophysica Acta.* 291:136–143.

Kefalides, N. A. 1973. Structure and biosynthesis of basement membranes. *International Review of Connective Tissue Research.* 6:63–104.

Kirsch, G. E., R. A. Nichols, and S. Nakajima. 1977. Delayed rectification in the transverse tubules. *Journal of General Physiology.* 70:1–21.

Liebman, P. A., and G. Entine. 1974. Lateral diffusion of visual pigment in photoreceptor disk membranes. *Science.* 185:457–459.

Miledi, R. 1960. The acetylcholine sensitivity of frog muscle fibres after complete or partial denervation. *Journal of Physiology.* 151:1–23.

Nagata, Y., and M. M. Burger. 1974. Wheat germ agglutinin: molecular characteristics and specificity for sugar binding. *Journal of Biological Chemistry.* 249:3116–3122.

Nicolson, G. L. 1974. The interactions of lectins with animal cell surfaces. *International Review of Cytology.* 39:89–190.

Oxford, G. S., and J. P. Pooler. 1975. Ultraviolet photoalteration of ion channels in voltage-clamped lobster axons. *Journal of Membrane Biology.* 20:13–30.

Ozanne, B., and J. Sambrook. 1971. Binding of radioactively labeled concanavalin A and wheat germ agglutinin to normal and virus-transformed cells. *Nature New Biology.* 232:156–160.

Peters, R., J. Peters, K. H. Tews, and W. Bahr. 1974. A microfluorimetric study of translational diffusion in erythrocyte membranes. *Biochimica et Biophysica Acta.* 367:282–294.

Poo, M.-M., and R. A. Cone. 1974. Lateral diffusion of rhodopsin in the photoreceptor membrane. *Nature.* 247:438–441.

Roberts, W. M., and W. Almers. 1985. Increased Na$^+$ current density near endplates in snake skeletal muscle. *Biophysical Journal.* 47:189a. (Abstr.)

Saffman, P. G., and M. Delbruck. 1975. Brownian motion in biological membranes. *Proceedings of the National Academy of Sciences.* 72:3111–3115.

Schwartz, L. M., E. W. McCleskey, and W. Almers. 1985. Dihydropyridine receptors in muscle are voltage dependent, but most are not functional calcium channels. *Nature.* 314:747–751.

Sigworth, F. J. 1980. The variance of sodium current fluctuations at the node of Ranvier. *Journal of Physiology.* 307:97–129.

Standen, N. B., P. R. Stanfield, T. A. Ward, and S. W. Wilson. 1984. A new preparation for

recording single-channel currents from skeletal muscle. *Proceedings of the Royal Society of London B Biological Sciences.* 221:455–464.

Stanfield, P. R. 1970. The effect of the tetraethylammonium ion on the delayed currents of frog skeletal muscle. *Journal of Physiology.* 209:209–229.

Stühmer, W., and W. Almers. 1982. Photobleaching through glass micropipettes: sodium channels without lateral mobility in the sarcolemma of frog skeletal muscle. *Proceedings of the National Academy of Sciences.* 79:946–950.

Stühmer, W., W. M. Roberts, and W. Almers. 1983. The loose patch clamp. *In* Single Channel Recording. B. Sakmann and E. Neher, editors. Plenum Publishing Co., New York. 123–132.

Tank, D. W., E. S. Wu, and W. W. Webb. 1982. Enhanced molecular diffusibility in muscle membrane blebs: release of lateral constraints. *Journal of Cell Biology.* 92:207–212.

Wakayama, Y., E. Bonilla, and D. L. Schotland. 1980. Ultrastructural localization of concanavalin A-binding sites in satellite cells of human skeletal muscle. *Cell Tissue Research.* 210:79–84.

Weiss, R. E., W. M. Roberts, W. Stühmer, and W. Almers. 1985. Potassium channel lateral mobility and photodestruction by ultraviolet light. *Biophysical Journal.* 47:384a. (Abstr.)

Weiss, R. E., W. Stühmer, and W. Almers. 1984a. Mobility of lectin receptors on frog muscle cell surface. *Biophysical Journal.* 45:269a. (Abstr.)

Weiss, R. E., W. Stühmer, and W. Almers. 1984b. Lateral diffusion characteristics of ionic channels and lectin binding sites in frog skeletal muscle membrane. *Abstracts of the 8th International Biophysics Congress.* 85.